Current Applied Science and Technology Vol. 21 No. 4 (October-December 2021)

Electrical Properties of Bistable Device Based on Graphene Oxide Composited with Polyvinylpyrrolidone Thin Films

Thutiyaporn Thiwawong, Potiyan Songkeaw, Korakot Onlaor* and Benchapol Tunhoo

Electronics and Control Systems for Nanodevices Research Laboratory,
College of Nanotechnology, King Mongkut's Institute of Technology Ladkrabang,
Bangkok, Thailand

Received: 3 November 2020, Revised: 17 February 2021, Accepted: 17 March 2021

Abstract

This research studied the bistable properties of synthesized graphene oxide (GO) composited with polyvinylpyrrolidone (PVP). The devices were fabricated using a spin coating process on indium tin oxide (ITO)/glass substrate, and the top electrodes were prepared by thermal evaporation with the device structure of ITO/PVP:GO/Al. The PVP:GO films were characterized by Raman spectroscopy, Fourier-transform infrared spectroscopy, X-ray photoemission spectroscopy, and scanning electron microscopy. The current-voltage (I-V) characteristics of the fabricated device exhibited a maximum ON/OFF current ratio in the order of about 10^4 at a GO concentration of 4 wt%. The mechanism was explained by fitting with the results of the I-V measurement. Moreover, the retention test of the device was more than 2×10^4 s. The device showed the important characteristics of memory to be a candidate for data storage.

Keywords: graphene oxide; memory device; polymer; composite; nanomaterials
DOI.....

1. Introduction

Graphene oxide (GO) is a family group of chemically modified graphene (CMG) materials [1]. Typically, GO can be synthesized by a chemical oxidation technique that can be prepared for mass scale production [2]. The structure of GO is composed of a graphene sheet to which various functional groups, such as carbonyl, hydroxyl, carboxylic groups and so on, are attached to the plane and edges of a graphene sheet [3]. Thus, the various physical properties of GO comprising electronic, optical, mechanical properties etc. depend on the order of the oxidization of the functional groups on the graphene sheet [4]. In recent years, studies in GO material have received much interest because of the numerous advantages like the simple preparation process and low cost. Moreover, GO was studied to be applied in various fields of application including sensors, energy storage, optoelectronic devices, etc. [5-7].

*Corresponding author: Tel.: (+66) 23298000 ext. 3128
E-mail: korakot.onlaor@gmail.com

For an electronics system, the memory device plays an important part for remembering the data in the system. A resistive random access memory device is a candidate of a novel memory device due to its exhibited advantageous properties including low operating voltage, high speed, simple fabrication process, etc. [8]. Bistable memory device can be prepared from various materials like nanoparticles, polymers, ceramics, and carbon-based materials. Bistable devices with a structure of nanoparticle-polymer composite materials have been extensively studied as they offer a variety of beneficial properties; e.g., simple fabrication and flexibility [9]. In this kind of device structure, the polymer acts as the host matrix for dispersal of nanoparticles. Many kinds of polymers could be used, such as poly (9-vinylcarbazole) (PVK), poly (methyl methacrylate) (PMMA), polyvinylpyrrolidone (PVP), etc. [10]. Among these, the PVP polymer was shown to be a dielectric polymer material with a large energy band gap that had a low cost and good thermal stability [11]. However, the PVP composites with the nanoparticles as a charge trap were reported to improve the performance of the bistable device [12]. Additionally, various materials; for example, ZnO [13], Cu_2ZnSnS_4 [14], multiwalled carbon nanotube [15], MoS_2 [16], and Co_9Se_8 quantum dots were composited with PVP to improve the performance of the device [17].

In this current study, synthesized GO particles were composited with PVP polymer to fabricate the bistable device with the structure of ITO/PVP:GO/Al. The electrical behavior and conduction mechanisms of the bistable device were studied and explained. The time retention measurement of the fabricated device was also presented.

2. Materials and Methods

Graphite powder (Arcos Organics, USA) was used as a precursor, and a modified Hummer's method [18] was used to synthesis the GO. The graphite powder was oxidized to produce GO that could be exfoliated into GO particles. First, the graphite powder, H_2SO_4 (96%), and $NaNO_3$ were mixed together at a ratio of 1 g: 50 ml: 1 g, respectively. The mixed solution was kept at a temperature below 20°C. After that, 6 g of $KMnO_4$ was slowly added to the mixed solution. Next, 70 ml of distilled water was added to the solution at a temperature of 90°C for two h. Finally, distilled water and H_2O_2 were added to stop the oxidized reaction. To collect the synthesized product, the GO particles were washed several times with distilled water and baked at 100°C until they became dry black particles.

To fabricate the bistable device, the PVP:GO solution was prepared by a fixed PVP concentration in ethanol at 70 mg/ml. The GO particles were added at 0%, 2%, 4%, and 6% by weight (wt%) of the PVP and ultrasonicated for 20 min for complete dispersion. A commercial indium tin oxide (ITO) on glass substrate was used as the bottom electrode. The ITO substrate was patterned with two parallel line masks of 3 mm in width. After etching the electrodes, the ITO substrate was cleaned with deionized water, methanol, acetone, and isopropanol in an ultrasonication bath for 15 min for each solvent. The PVP:GO active layer was fabricated by spin coating with speed conditions of 500 rpm for 3 s and 1,500 rpm for 10 s, respectively. After the spinning process, the prepared film was baked at 50°C for one h. The top electrodes were 100 nm thick aluminum that was prepared by thermal evaporation in a high vacuum. Figure 1 depicts the schematic structure of the device.

The thickness of the PVP:GO films was measured as cross-section images from a field emission scanning electron microscope (FESEM, JEOL JSM-7001F). The properties of the PVP:GO composite films were evaluated using a Raman spectrophotometer (DXR smart Raman, Thermo scientific) with 532 nm of an exciting light source, Fourier-transform infrared spectroscopy (FTIR) analysis in UTR mode (Thermo and Perkin Elmer), and X-ray photoelectron

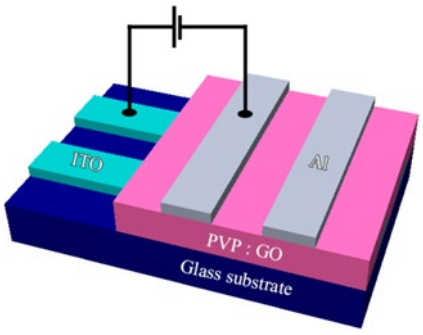

Figure 1. The structure of the ITO/PVP:GO/Al device

spectroscopy (XPS, AXIS Ultra DLD, Kratos), respectively. The electrical properties of the device were measured in terms of the current-voltage (I-V) characteristics and time retention test by a precision source meter (Keithley 2410).

3. Results and Discussion

Raman spectroscopy is a non-destructive characterization technique for carbon family materials, which can be used to confirm the structure of synthesized GO materials [19]. Figure 2a depicts the three components in the Raman spectrograph of the GO particles. The observed peak positions at 1350, 1580, and 2924 cm^{-1} could be assigned to the D peak from the sp^3 defect, G peak from sp^2 in the carbon bonding, and 2D band of the graphene sheet [19], respectively. The intensity ratio of the D/G peaks was 0.89, which confirmed the synthesized GO in this study [20-22]. Moreover, the intensity ratio of the 2D/G peaks was 0.08, which was related to the multilayered synthesized GO sheet [20, 21].

FTIR was used to characterize the function groups of the PVP:GO layer; an example result from the PVP:GO 4 wt% is shown in Figure 2b. The absorption band at 3406 cm^{-1} was assigned to the O-H stretching vibration due to the water molecule absorption of the materials [23]. The absorption band at 2940 cm^{-1} was assigned to C-H and corresponds to asymmetric stretching vibration of the vinyl groups in the PVP. The absorption peak at 1279 cm^{-1} and 1647 cm^{-1} could be assigned to the C-N vibration and C=O stretching vibration in the pyrrolidone ring of the PVP molecule. The absorption peak at 1433 cm^{-1} was assigned to the CH_2 bending vibration of the PVP polymer [24, 25]. In the case of the PVP:GO layer, these peaks exhibited higher intensity, which was proportional to the concentrate of the GO. In addition, the other absorption peaks at 1080 cm^{-1} and 1377 cm^{-1} could be assigned to the C-O vibration of the alkoxy and epoxy function groups, respectively. The FTIR confirmed the composite materials of the PVP and GO.

XPS is a technique for determining the elements and composition of the material. A high resolution spectrograph of the C1s and O1s components from the PVP:GO 4wt% is shown in Figures 2c-2d. These peaks were fitted with Lorentz-Gaussian distribution functions. The O1s peak exhibited three components with binding energies of 530.70, 531.70, and 532.62 eV, respectively, which were identified as C=O, C-O, and O-H bonds, respectively [26, 27]. It was observed that the high intensity of the C-O and O-H peaks could confirm the composited material with the PVP and GO. Simultaneously, the C1s peak showed four components that had binding energies of 284.49, 285.44, 287.16, and 288.15 eV, respectively, which could be identified as the C-C, C-N, C-O, and C=O bonds, respectively [26-29].

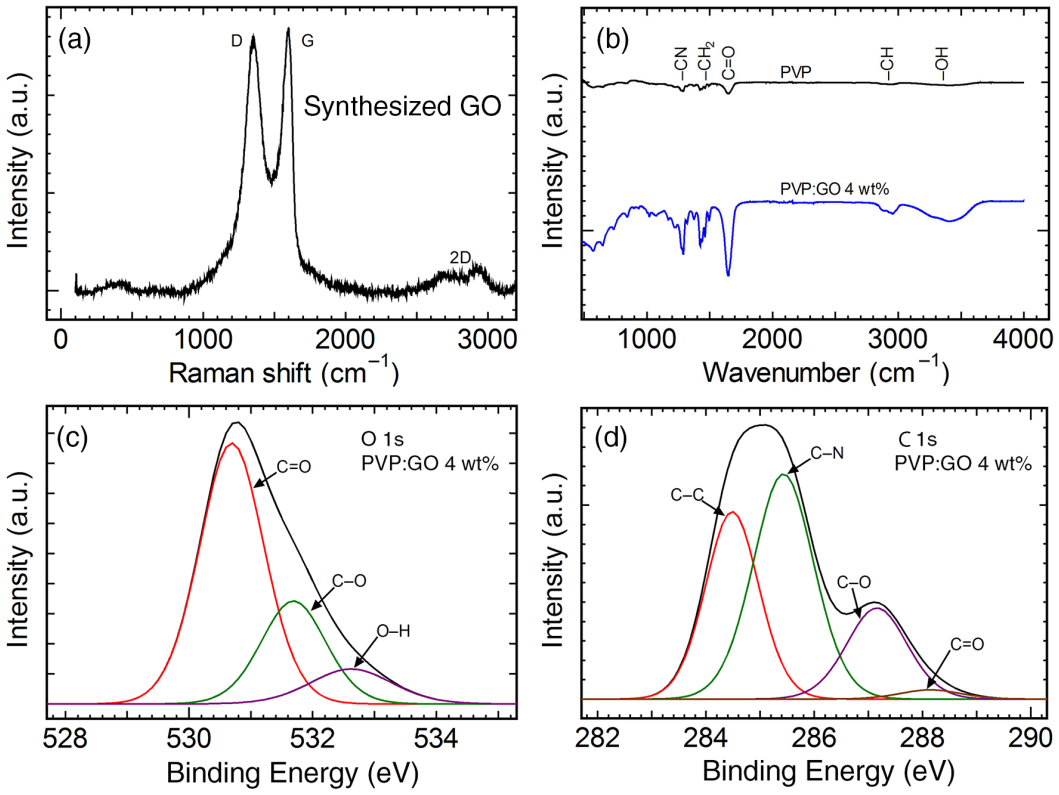

Figure 2. (a) Raman spectrogram of the synthesized GO particles; (b) FTIR spectrogram of the PVP:GO 4wt% layer. The high resolution XPS spectrogram of the PVP:GO 4wt% layer at (c) O 1s and (d) C 1s.

A cross-section scanning electron microscope was used to obtain the thickness of the prepared films (Figure 3). The direct estimate from the images represented the thicknesses of the PVP and PVP:GO at 121.14±13.19 and 111.20±5.35 nm, respectively (measured in 10 randomly selected cross-section points, and the thicknesses are average values with standard deviations). The thicknesses of the films were quite uniform throughout the films. In the case of the ITO electrode, the thickness was 155±20 nm (data from Xinyan Technology Ltd.) whereas the 100 nm-thick Al electrodes of all devices were prepared under the same conditions and monitored by a high-resolution thickness monitor (XTC/2, INFICON).

The electrical properties of the device were assessed with I-V measurement. Applied voltage was swept from 0 V to +5 V for Step 1, +5 V to -5 V for Step 2, and -5 V to 0 V for Step 3. Figure 4 depicts the relationship between the current and voltage. For the 2 wt% and 4 wt% of the GO concentrations, the results exhibited two states of current that were defined as low current (OFF state) and high current (ON state). In the case of only the PVP layer, the ratio of the current of the ON state and OFF state (ON/OFF ratio) was small, as the applied voltage into the device was not sufficient to change the electrical conduction of the PVP polymer. Furthermore, at 2 wt% of GO concentration in the film, the hysteresis loops of the device still showed a small hysteresis, as shown in the inset of Figure 4. The highest ON/OFF ratio was observed at the GO concentration of 4 wt% with a writing voltage of +5 V, a reading voltage of +1 V and the ON/OFF current ratio

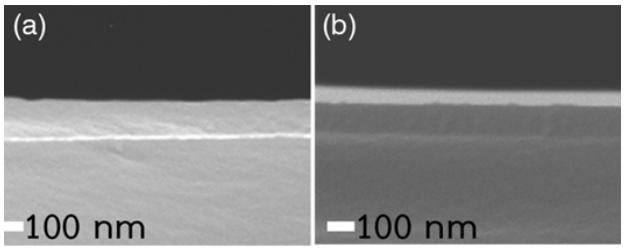

Figure 3. Cross-section SEM images of (a) PVP on the glass substrate, and (b) PVP:GO 4 wt% on the glass substrate

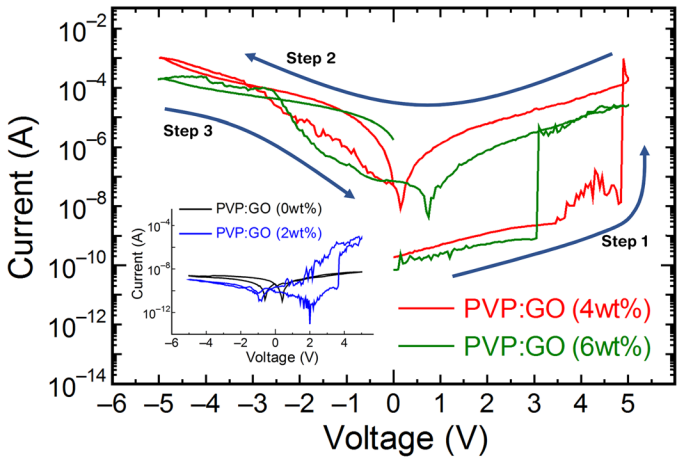

Figure 4. I-V characteristics of the memory device with different GO concentrations

of approximately 10^4. Moreover, the I-V curve characteristics remained in the ON state although a negative bias voltage was applied. The behavior of the device indicated the characteristic of a write-once-read-many (WORM) memory device. However, when the concentration of the GO is increased to 6 wt%, the switching voltage and ON/OFF current ratio went down, and the effect of GO concentration is discussed in the next section.

The ITO/PVP:GO (4 wt%)/Al device showed optimal memory properties with the highest ON/OFF current ratio of memory device. Therefore, to explain the conduction mechanisms of the device, the I-V curves of the GO 4wt% were fitted with an electrical conduction model. The fitted curve was optimized with the models of thermionic emission (TE) and space charge limited current (SCLC).

First, TE had the expression as [30]:

$$I \propto T^2 \exp\left[\frac{-(\phi_b - q\sqrt{qV/4\pi d\varepsilon_i})}{k_b T}\right] \quad (1)$$

where T is the absolute temperature, q is the charge constant, ϕ_b is the barrier height, ε_i is the insulator permittivity, and kb is the Boltzmann's constant. The equation could be rearranged with a linear equation between $\ln(I) \propto V^{1/2}$. The SCLC had the expression as follows:

$$I \propto V^{\alpha} \quad (2)$$

Where α is constant with α = 1 is Ohmic conduction
α = 2 is SCLC
α ≫ 2 is the trap filled limit of SCLC.

In the OFF state, the dominating conduction was the thermal injection over the barrier that corresponded to the TE model (Figure 5a). In the ON state, the electrical models changed to SCLC with the slope of the curve corresponding to α = 2.35 (Figure 5b). The theoretical trap free SCLC showed α = 2, so, α more than 2 should affect the trap fill SCLC [31]. This could imply that the GO acts like a carrier trap [31] in the PVP.

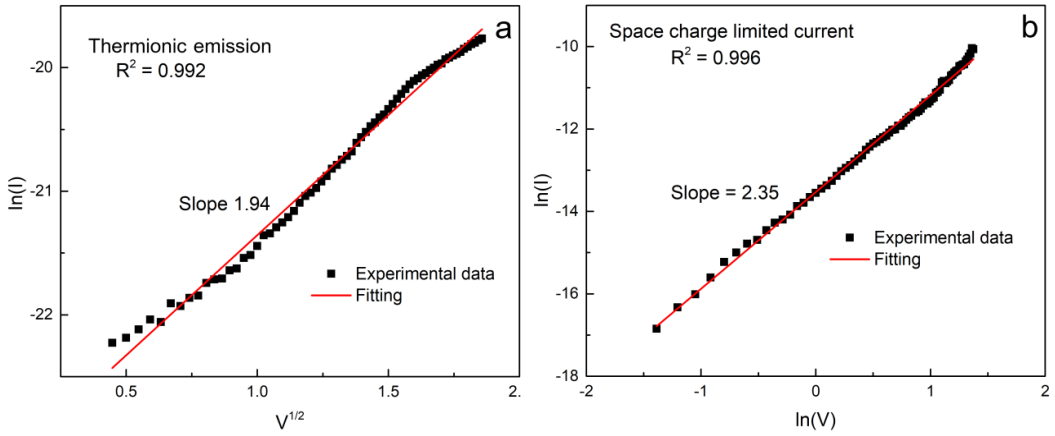

Figure 5. I-V curves fitting of the ITO/PVP:GO (4 wt%)/Al device
(a) TE mechanism at the OFF state and (b) SCLC mechanism at the ON state

To explain more about the behavior of the device, the mechanism models of ITO/PVP:GO/Al were proposed in terms of the energy band diagram. In other studies [32], the LUMO and HOMO energy levels of the PVP material were located at -2.01 and -5.93 eV, respectively. For the GO material, the energy levels also depended on the structure of the GO. Kim *et al*. [33] reported on the estimated conduction and valence energy levels of the GO and rGO in ranges of -2.245 to -2.525 eV and -5.445 to -5.115 eV. Those values were closer when the GO was reduced to become the rGO. Liu *et al*. [34] reported on the value of the GO ribbon with the LUMO and HOMO levels that were located at -3.5 and -5.3 eV, respectively. It could be seen that the conduction level of the GO and rGO was also lower than the LUMO level of the PVP. On the other hand, the valence levels of the GO and rGO were also higher than the HOMO level of the PVP. Therefore, Figure 6a depicts the proposed models of the device. First, the electrons were injected through the barrier from the Al electrode into the PVP:GO layer due to thermal injection that resulted from the TE model in the OFF state (Figure 6b). After that, when the GO trapping states were filled by the electrons, the device changed to the ON state, which corresponded to the trap filled limit SCLC (Figure 6c). The electrons could be released from the PVP:GO layer although a negative voltage was applied because of the trapped electrons in the layer and the injected electrons from the electrode (Figure 6d). Therefore, the devices maintained the ON state with a small drop of current due to the effect of the barrier height between the positive and negative voltages.

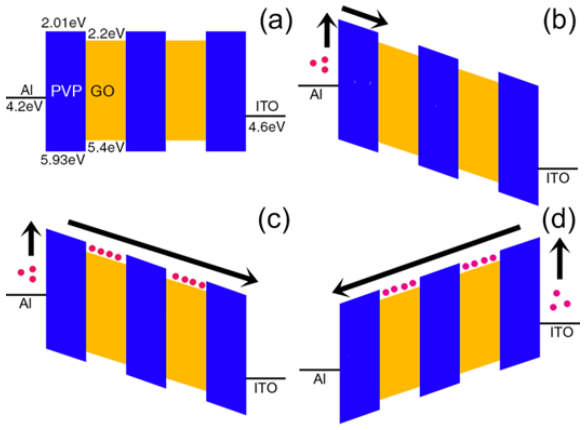

Figure 6. Schematic energy band diagram of the GO blend in PVP at 4 wt% corresponding to the carrier trap mechanism of (a) 0 V, (b) OFF state, (c) ON state, and (d) negative voltage

Moreover, the GO concentration had an effect on the conduction of the device. For the condition of the mechanism of the GO 4-6 wt%, the devices might have a shorter width barrier of PVP due to the PVP being separated by the GO resulting in the electrons being easier to be injected by thermal energy across the interface barrier between the ITO and PVP. However, the higher barrier height at the interface led to the low conduction of the device; the hypothesis could be supported by the negative voltage when the electrons were injected from the ITO electrode.

In addition, the time retention characteristic was shown to be an important parameter of the bistable device [35, 36]. This characteristic could be demonstrated in the retention of the GO 4wt% composites PVP device in both the ON and OFF states for various long periods of time measurement. The test was performed with a continuous reading at +1 V every 300 ms to acquire the retention of the OFF state. After that, a voltage pulse of +5 V was applied to the device as a writing process. Then, the device was continuously read at +1 V every 300 ms to acquire the retention of the ON state. Figure 7 depicts the retention characteristic of the GO composite PVP device. It could be seen that the device exhibited more retention time at 2×10^7 seconds with the ON/OFF ratio still remaining about 10^4. The fluctuation of the current states might have been due to the effect of the charge disturbance of the low current. However, the ON/OFF current ratio was still higher than 10^4, which ensured protecting against the misreading process [37].

In comparison with previous studies, the summary of the GO composite bistable device is shown in Table 1. Liu *et al*. [38] reported on the resistive switching characteristics of the graphene oxide-polypyrrole-polyvinylferrocene ternary nanocomposite for which the device exhibited an ON/OFF current ratio of 10^3 and time retention stability over a period of 5,000 s. Khuran *et al*. [39] demonstrated the flexibility of the resistive random access memory of zinc oxide nanorods incorporating GO sheets. That device had an ON/OFF ratio of about 100 with an endurance cycle of over 200 cycles. Kim *et al*. [40] reported the resistive switching behavior of the PVA/GO+PVA composite/PVA. That device demonstrated an ON/OFF ratio of about 10^4 with a retention time of 2×10^3 s. It could be seen that the bistable device based on the structure of the GO and PVP composites exhibited appropriate performances of bistable behavior for a resistive random access memory device.

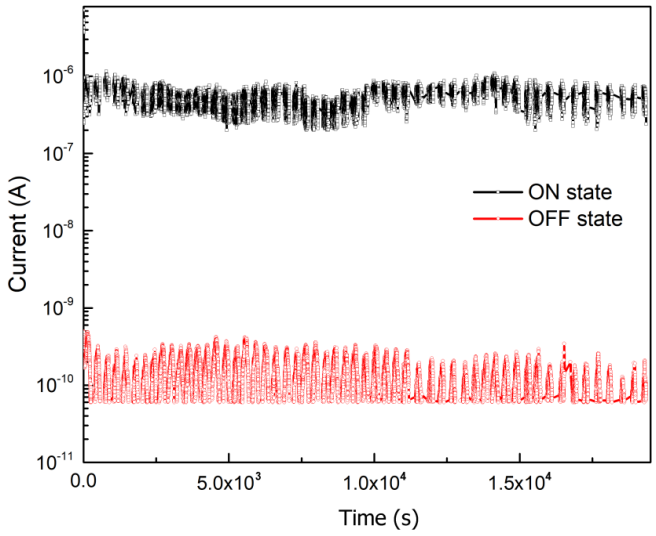

Figure 7. The retention time of the reading data at 1 V of the PVP:GO 4 wt% condition.

Table 1. Summary of the bistable device based on the polymer-GO thin films

Structure	**ON/OFF ratio**	**Retention time (s)**	**Reading voltage (V)**	**Mechanism**	**Ref.**
ITO/GO–PyVf/Al	10^3	$>5\times10^3$	+0.1	trapping	[38]
Al/GOZNs/ITO	10^2	$>10^4$	+0.1	filamentary	[39]
PVA/GO+PVA/PVA	10^4	$>2\times10^3$	+1	filamentary	[40]
Al/PTPEB-g-RGO/ITO	10^4	$>10^4$	+0.1	trapping	[41]
Al/PAE-g-RGO/ITO	10^3	$>10^4$	-1	trapping	[42]
ITO/PMMA-GOs/Al	10^4	$>10^4$	N/A	trapping	[43]
Al/PVP-GO/ITO	10^4	$>10^4$	+1	trapping	This work

4. Conclusions

A bistable device based on composite films of GO and PVP was fabricated with a device structure of ITO/PVP:GO/Al. The current-voltage characteristics of the device demonstrated non-volatile WORM memory behavior. The conduction mechanisms based-on TE and SCLC in the OFF and ON states were observed from the I-V fitting model, respectively, with the GO acting to create trapping states in the composites film. The optimized current ON/OFF ratio was observed to be in the order of about 10^4 from the GO concentration of 4 wt% with +1 V reading voltage. Moreover, the retention time of device was more than 2×10^4 s for each state.

5. Acknowledgements

This work was supported by King Mongkut's Institute of Technology Ladkrabang (grant number: KREF146203). The authors acknowledge the facilities, and technical assistance from Nanotechnology and Materials Analytical Instrument Service Unit (NMIS) of College of Nanotechnology, King Mongkut's Institute of Technology Ladkrabang.

References

[1] Zhu, Y., Murali, S., Cai, W., Li, X., Suk, J.W., Potts, J.R. and Ruoff, R.S., 2011. Graphene and graphene oxide: Synthesis, properties, and applications. *Advanced Materials*, 22, 3906-3924.

[2] Gómez-Navarro, C., Meyer, J.C., Sundaram, R.S., Chuvilin, A., Kurasch, S., Burghard, M., Kern, K. and Kaiser, U., 2010. Atomic structure of reduced graphene oxide. *Nano Letters,* 10, 1144-1148.

[3] Ban, F.Y., Majid, S.R., Huang, N.M. and Lim, H.N., 2012. Graphene oxide and its electrochemical performance. *International Journal of Electrochemical Science*, 7, 4345-4351.

[4] Panin, G.N., Kapitanova, O.O., Lee, S.W., Baranov, A.N. and Kang, T.W., 2011. Resistive switching in Al/graphene oxide/Al structure. *Japanese Journal of Applied Physics*, 50, 070110, https://doi.org/10.1143/JJAP.50.070110

[5] Maccaferri, G., Terzi, F., Xia, Z., Vulcano, F., Liscio, A., Palermo, V. and Zanardi, C., 2019. Highly sensitive amperometric sensor for morphine detection based on electrochemically exfoliated graphene oxide. Application in screening tests of urine samples. *Sensors and Actuators B: Chemical*, 281, 739-745.

[6] Ye, M., Gao, J., Xiao, Y., Xu, T., Zhao, Y. and Qu, L., 2017. Metal/graphene oxide batteries. *Carbon*, 125, 299-307.

[7] Santiago, S.R.M.S., Chang, C.-H., Lin, T.-N., Yuan, C.-T. and Shen, J.-L., 2019. Diethylenetriamine-doped graphene oxide quantum dots with tunable photoluminescence for optoelectronic applications. *ACS Applied Nano Materials*, 2, 3925-3933.

[8] Hong, S.K., Kim, J.E., Kim, S.O., Choi, S. and Cho, B.J., 2010. Flexible resistive switching memory device based on graphene oxide. *IEEE Electron Device Letters*, 31, 1005-1007.

[9] Son, D.-I., Park, D.-H., Choi, W.K., Cho, S.-H., Kim, W.-T. and Kim, T.W., 2009. Carrier transport in flexible organic bistable devices of ZnO nanoparticles embedded in an insulating poly(methyl methacrylate) polymer layer. *Nanotechnology*, 20, 195203.

[10] Marsden, A.J., Papageorgiou, D.G., Vallés, C., Liscio, A., Palermo, V., Bissett, M.A., Young, R.J. and Kinloch, I.A., 2018. Electrical percolation in graphene-polymer composites. *2D Materials*, 5(3), 032003, https://doi.org/10.1088/2053-1583/aac055

[11] Huang, S., Zhou, L., Li, M.-C., Wu, Q., Kojima, Y. and Zhou, D., 2016. Preparation and properties of electrospun poly(vinyl pyrrolidone)/cellulose nanocrystal/silver nanoparticle composite fibers. *Materials*, 9(7), 523, https://doi.org/10.3390/ma9070523

[12] Gu, C., Mao, H.-W., Tao, W.-Q., Zhou, Z., Wang, X.-J., Tan, P., Cheng, S., Huang, W., Sun, L.-B., Liu, X.-Q., Liu, X.-Q. and Liu, J.-Q., 2019. Facile synthesis of $Ti_3C_2T_x$–Poly(vinylpyrrolidone) nanocomposites for nonvolatile memory devices with low switching voltage. *ACS Applied Materials & Interfaces*, 11, 38061-38067.

[13] Onlaor, K., Thiwawong, T. and Tunhoo, B., 2014. Electrical switching and conduction mechanisms of nonvolatile write-once-read-many-times memory devices with ZnO nanoparticles embedded in polyvinylpyrrolidone. *Organic Electronics*, 15, 1254-1262.

[14] Kim, Y.N., Yun, D.Y., Arul, N.S. and Kim, T.W., 2015. Carrier transport mechanisms of multilevel nonvolatile memory devices with a floating gate consisting of hybrid organic/ inorganic nanocomposites. *Organic Electronics*, 17, 270-274.

[15] Kim, W.T., Jung, J. H. and Kim, T.W., 2009. Carrier transport mechanisms in nonvolatile memory devices fabricated utilizing multiwalled carbon nanotubes embedded in a poly-4-vinyl-phenol layer. *Applied Physics Letters*, 95(2), 022104, https://doi.org/10.1063/1. 3174913

[16] Wu, Z., Wang, T., Sun, C., Liu, P., Xia, B., Zhang, J., Liu, Y. and Gao, D., 2017. Resistive switching effect of N-doped MoS_2-PVP nanocomposites films for nonvolatile memory devices. *AIP Advances*, 7(12), 125213, https://doi.org/10.1063/1.4994227

[17] Zhang, P., Xu, B., Gao, C., Chen, G. and Gao, M., 2016. Facile synthesis of Co_9Se_8 quantum dots as charge traps for flexible organic resistive switching memory device. *ACS Applied Materials & Interfaces*, 8, 30336-30343.

[18] Yu, H., Zhang, B., Bulin, C., Li, R. and Xing, R., 2016. High-efficient Synthesis of Graphene Oxide Based on Improved Hummers Method. *Scientific Reports*, 6, 36143, https://doi.org/10.1038/srep36143

[19] Wu, J.-B., Lin, M.-L., Cong, X., Liu, H.-N. and Tan, P.-H., 2018. Raman spectroscopy of graphene-based materials and its applications in related devices. *Chemical Society Reviews*, 47, 1822-1873.

[20] Khan, Q.A., Shaur, A., Khan, T.A., Joya, Y.F. and Awan, M.S., 2017. Characterization of reduced graphene oxide produced through a modified Hoffman method. *Cogent Chemistry*, 3, 1298980, https://doi.org/10.1080/23312009.2017.1298980

[21] Kim, H.J., Lee, S.-M., Oh, Y.-S., Yang, Y.-H., Lim, Y.S., Yoon, D.H., Lee, C., Kim, J.-Y. and Ruoff, R.S., 2014. Unoxidized graphene/alumina nanocomposite: Fracture- and wear-resistance effects of graphene on alumina matrix. *Scientific Reports*, 4, 5176, https:// doi.org/10.1038/srep05176

[22] Ray, S.C., Bhunia, S.K., Saha, A. and Jana, N.R., 2015. Graphene oxide (GO)/reduced-GO and their composite with conducting polymer nanostructure thin films for non-volatile memory device. *Microelectronic Engineering*, 146, 48-52.

[23] Abdelghany, A.M., Mekhail, M.S., Abdelrazek, E.M. and Aboud, M.M., 2015. Combined DFT/FTIR structural studies of monodispersed PVP/gold and silver nano particles. *Journal of Alloys and Compounds*, 646, 326-332.

[24] Koczkur, K.M., Mourdikoudis, S., Polavarapu, L. and Skrabalak, S.E., 2015. Polyvinylpyrrolidone (PVP) in nanoparticle synthesis. *Dalton Transaction*, 44, 17883-17905.

[25] Song, Y.J., Wang, M., Zhang, X.Y., Wu, J.Y. and Zhang, T., 2014. Investigation on the role of the molecular weight of polyvinyl pyrrolidone in the shape control of high-yield silver nanospheres and nanowires. *Nanoscale Research Letters*, 9, 17, https://doi.org/10.1186/ 1556- 276X-9-17

[26] Zang, L., Cao, X., Zhang, Y., Sun, L., Qinb, C. and Wang, C., 2015. Microfluidic generation of graphene beads for supercapacitor electrode materials. *Journal of Materials Chemistry A*, 3, 22088-22093.

[27] Cheng, D., Xie, R., Tang, T., Jia, X., Cai, Q. and Yang, X., 2016. Regulating micro-structure and biomineralization of electrospun PVP-based hybridized carbon nanofibers containing bioglass nanoparticles via aging time. *RSC Advances*, 6, 3870-3881.

[28] Li, S.K., Yan, Y.X., Wang, J.L. and Yu, S.H., 2013. Bio-inspired in situ growth of monolayer silver nanoparticles on graphene oxide paper as multifunctional substrate. *Nanoscale*, 5, 12616-12623.

[29] Wang, Z.-L., Yan, J.-M., Zhang, Y.-F., Ping, Y., Wanga, H.-L. and Jianga, Q., 2014. Facile synthesis of nitrogen-doped graphene supported AuPd-CeO_2 nanocomposites with high-performance for hydrogen generation from formic acid at room temperature. *Nanoscale*, 6(6), 3073-3077.

[30] Chen, K.H., Tsai, T.M., Cheng, C.M., Huang, S.J., Chang, K.C., Liang, S.P. and Young, T.F., 2018. Schottky emission distance and barrier height properties of bipolar switching Gd:SiO_x RRAM devices under different oxygen concentration environments. *Materials*, 11, 43, https://doi.org/10.3390/ma11010043

[31] Ikuno, T., Okamoto, H., Sugiyama, Y., Nakano, H., Yamada, F. and Kamiya, I., 2011. Electron transport properties of Si nanosheets: Transition from direct tunneling to Fowler-Nordheim tunneling. *Applied Physics Letters*, 99, 023107, https://doi.org/10.1063/1.3610486

[32] Yu, X., Yu, X., Zhang, J., Zhang, D., Caib, H. and Zhao, Y., 2015. Interfacial modification for improving inverted organic solar cells by poly(N-vinylpyrrolidone). *RSC Advances*, 5, 58966-58972.

[33] Kim, J., Ganorkar, S., Kim, Y.H. and Kim, S.I., 2015. Graphene oxide hole injection layer for high-efficiency polymer light-emitting diodes by using electrophoretic deposition and electrical reduction. *Carbon*, 94, 633-640.

[34] Liu, J., Xue, Y., Gao, Y., Yu, D., Durstock, M. and Dai, L., 2012. Hole and electron extraction layers based on graphene oxide derivatives for high-performance bulk heterojunction solar cells. *Advanced Materials*, 24, 2228-2233.

[35] Zhang, X., Xu, J., Zhang, X., Shi, S., Zhao, X. and Li, L., 2017. Electrical bistable properties of nonvolatile memory device based on hybrid ZCIS NCs: PMMA film. *Materials Science in Semiconductor Processing*, 57, 105-109.

[36] Huang, J., Zhao, X., Zhang, H., Bai, J., Wang, S., Wang, C., Mad D. and Hou, Y., 2019. Flash memory devices and bistable nonvolatile resistance switching properties based on PFO doping with ZnO. *RSC Advances*, 9, 9392-9400.

[37] Ling, Q.D., Liaw, D.J., Teo, E.Y.H., Zhu, C., Chan, D.S.H., Kang, E.T. and Neoh, K.G., 2007. Polymer memories: Bistable electrical switching and device performance. *Polymer*, 48, 5182-5201.

[38] Liu, R., Ni, X. and Lin, J., 2019. Preparation of graphene oxide-polypyrrole-polyvinylferrocene ternary nanocomposite and its resistive-switching characteristic. *Journal of Materials Science: Materials in Electronics*, 30, 1001-1008.

[39] Khurana, G., Misra, P., Kumar, N. and Katiyar, R.S., 2014. Tunable power switching in nonvolatile flexible memory devices based on graphene oxide embedded with ZnO nanorods. *Journal of Physical Chemistry C*, 118, 21357-21364.

[40] Kim, T., Kim, D.K., Kim. J. and Pak, J.J., 2019. Resistive switching behaviour of multi-stacked PVA/graphene oxide + PVA composite/PVA insulating layer-based RRAM devices. *Semiconductor Science and Technology*, 34, 065006, https://doi.org/10.1088/1361-6641/ab1403

[41] Cao, Y., Fu, Y., Li, D., Zhu, C., Zhang, B. and Chen, Y., 2019. Organophosphorus-based polymer covalently functionalized reduced graphene oxide: In-situ synthesis and nonvolatile memory effect. *Carbon*, 141, 758-767.

[42] Sun, S., Zhuang, X., Liu, B., Wang, L., Gu, L., Song, S., Zhang, B. and Chen, Y., 2016. In situ synthesis and characterization of poly(aryleneethynylene)-grafted reduced graphene oxide. *Chemistry-A European Journal*, 22, 2247-2252.

[43] Gogoi, K.K. and Chowdhury, A., 2019. Electric field induced tunable memristive characteristics of exfoliated graphene oxide embedded polymer nanocomposites, *Journal of Applied Physics*, 126, 025501, https://doi.org/10.1063/1.5102145